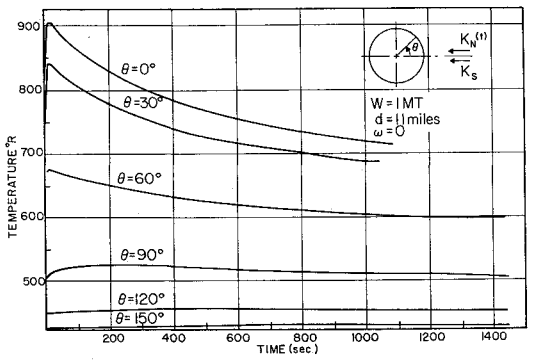

Fig. 2 Temperature distribution in a nonrotating cylinder.

with the constant N given as

$$N = P_{\max}/4\pi d^2$$

$P_{\max}$ is the maximum radiative power of the weapon, and t_M is the time required to achieve that value. The distance from the cylindrical shell to the weapon is given by d.

For the curve fit, the value $\delta_1 = 0.35$ was chosen to give proper behavior as $t \to \infty$. The values of G_j are $G_1 = 0.574$, $G_2 = 0.090$, $G_3 = 39.181$, $G_4 = -146.052$, $G_5 = 176.776$, and $G_6 = -70.568$.

Using Eq. (17), the coefficients $a_n(t)$ and $b_n(t)$ can be evaluated by quadrature of Eqs. (15) and (16):

$$a_n(t) = \sum_{j=1}^{6} \frac{G_j}{(\beta n^2 + \alpha - \gamma_j)^2 + n^2\omega^2} \times \{e^{(\beta n^2+\alpha-\gamma_j)t}\,[(\beta n^2 + \alpha - \gamma_j)\cos n\omega t + n\omega \sin n\omega t] - (\beta n^2 + \alpha - \gamma_j)\} \quad (18)$$

$$b_n(t) = \sum_{j=1}^{6} \frac{G_j}{(\beta n^2 + \alpha - \gamma_j)^2 + n^2\omega^2} \times \{e^{(\beta n^2+\alpha-\gamma_j)t}\,[(\beta n^2 + \alpha - \gamma_j)\sin n\omega t - n\omega \cos n\omega t] + n\omega\} \quad (19)$$

where

$$\gamma_j = \frac{\delta_1(3j-2)}{t_M} \qquad \beta n^2 + \alpha - \gamma_j \neq 0$$

The parameters describing the cylindrical shell were chosen as $r = 1$ ft, $s = \frac{1}{200}$ ft, $k = 100$ Btu/ft hr°R, $k\rho/c = 3$ ft²/hr, and $K_s = 442$ Btu/ft²hr. From this follows: $T_0 = 535.1$ °R, $\alpha = 0.00175$ sec^{-1}, and $\beta = 0.000833$ sec^{-1}.

Specifying a 1-megaton weapon, the formulas of Ref. 3 give $P_{\max} = 126.5 \times 10^{12}$ cal/sec and $t_M = 1$ sec. Further, choosing $d = 11$ miles gives $\mu = 0.0422$ sec^{-1}. With these numerical values the temperature distribution was computed for three special cases.

For the case of zero speed ($\omega = 0$), the temperature distribution was computed and plotted in Fig. 2 for several values of angle θ. At time zero, the distribution is that given by Ref. 1 for solar heating at zero speed.

For the case of very high speed ($\omega \to \infty$), the initial temperature is uniform, i.e., $T_s = T_0 = 535.1$ °R. The temperature variation with time is identical for all positions ψ on the cylinder. This variation is plotted in Fig. 3.

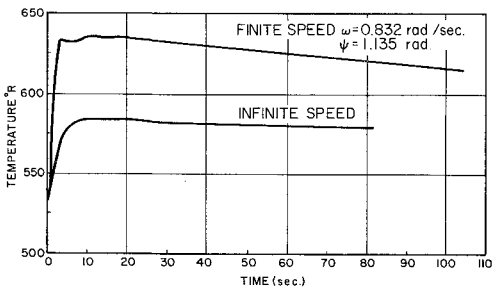

Fig. 3 Temperature distribution in a rotating cylinder.

For the case of finite speed ($\omega = 0.832$ rad/sec), the initial temperature distribution is still essentially uniform. The point on the cylinder which attains the highest temperature is located initially by $\psi = 1.135$ rad. The temperature history of this position is given in Fig. 3.

References

[1] Charnes, A. and Raynor, S., "Solar heating of a rotating cylindrical space vehicle," ARS J. **30**, 479–484 (1960).

[2] Olmstead, W. E. and Raynor, S., "Solar heating of a rotating spherical space vehicle," Intern. J. Heat Mass Transfer **5**, 1165–1177 (1962).

[3] Glasstone, S., "The effects of nuclear weapons," U. S. Dept. Defense, U. S. Atomic Energy Commission, U. S. Government Printing Office: 1957 0-424278 (June 1957).

Sphere of Influence in Patched-Conic Methods

JACK W. CRENSHAW*
General Electric Company, Daytona Beach, Fla.

THE so-called "patched-conic" method as an approximation of space trajectories is well known and widely used. In this method, each portion of the trajectory is treated as a two-body trajectory about the most influential body. At some point on a trajectory between two attracting bodies, these two bodies are equally influential, and the locus of such points is a roughly spheroidal surface. This surface is called the "sphere of influence," although, as will be seen, it is not truly spherical.

At this sphere of influence, a transition is made from one attracting body to the other by matching the relative position and velocity in the appropriate conic trajectories. Obviously, the choice of the surface at which the matching takes place is important to the overall result. A philosophy for choosing this surface can be developed by considering the desired end result: that the errors be minimized. This criterion can be stated mathematically, and other authors[1–3] have derived the approximate surface that results. (For the most complete such derivation, see Plummer.[9]) For practical reasons, the resulting spheroid almost always is further approximated by a sphere.[4–8,10]

If one is to use the patched-conic method with confidence, it is imperative that one be able to place bounds on the errors incurred. This means that one must examine each simplifying assumption and its effect. One such assumption is that of the shape of the sphere of influence, and for this reason an exact determination of its shape is desirable.

In studying the patched conic method, one need consider only three bodies at a time, since the sphere of influence always is determined by the two major attracting bodies. Figure 1 shows a three-body system (M_1, M_2, V) that is restricted only in the sense that the mass of the vehicle V is assumed negligible. It is assumed that the mass M_1 is greater than M_2. The radius vector convention uses capital letters to denote vectors from M_1 and lower case letters to denote those from M_2. The angle θ is defined by the dot product

$$\bar{r} \cdot \bar{R}_2 = -rR_2 \cos\theta \qquad 0 \leq \theta \leq \pi \quad (1)$$

Received April 15, 1963.

* Physicist, Flight Dynamics, Apollo Support Department. Member AIAA.

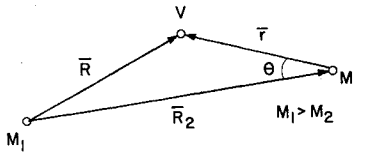

Fig. 1 Three-body system (M_1, M_2, V).

In general, the equations of motion of the vehicle are given by

$$\ddot{\bar{R}} = \bar{C}_1 + \bar{P}_2 \tag{2}$$

or

$$\ddot{\bar{r}} = \bar{C}_2 + \bar{P}_1 \tag{3}$$

where the $\bar{C}_i$'s are the central inverse-square forces of the form $-GM(\bar{R}/R^3)$, and the $\bar{P}_i$'s are perturbing forces of the form $-GM[(\bar{R}/R^3) - (\bar{R}_2/R_2^3)]$. In the patched-conic method the latter forces are ignored, and an error then is incurred proportional to the ratio P/C. If the sphere of influence is to be chosen so as to minimize the error, it should be defined as the locus of vectors $\bar{r}_s$ such that the ratios P_1/C_2 and P_2/C_1 are equal. Plummer and others have shown that the foregoing criterion leads to the following equation:

$$\rho = k^{2/5}$$

where

$$\rho = r_s/R_2 \qquad k = M_1/M_2 \tag{4}$$

The author has shown in Ref. 11 that the exact relation is

$$\rho^{10} = \frac{k^4(1 + Q)^{10/3}[1 + \rho^2(\rho^2 - 2\cos\theta)]}{1 + Q/\rho(Q/\rho + 2\cos\theta)} \tag{5}$$

where

$$Q = \frac{3}{2}x + \frac{3.1}{2.4}x^2 - \frac{3.1.1}{2.4.6}x^3 + \frac{3.1.1.3}{2.4.6.8}x^4 - \ldots \tag{6}$$

and

$$X = \rho(\rho - 2\cos\theta) \tag{7}$$

[Note that the series Q is defined by the relation $R^3 = R_2^3(1 + Q)$, which is found to be useful in evaluating perturbations. The series is similar in form and function to Encke's series.] An inspection of the equations will show the following:

1) Equations (5–7) must be solved simultaneously for ρ by iteration.

2) However, the form of Eq. (5) is such that the right-hand side is only weakly dependent on ρ if ρ is small, which suggests rapid convergence.

3) The definition used for θ [see Eq. (1)] requires that the sphere of influence be a body of revolution about the vector $\bar{R}_2$, and its shape is, therefore, independent of orientation of the orbital plane.

If, at this point, one assumes that $k \ll 1$, it can be shown that (5) reduces to $\rho = Ck^{2/5}$, where

$$C = (1 + 3\cos^2\theta)^{-1/10} \tag{8}$$

The minimum value of C occurs at $\theta = 0$ and is $4^{-1/10}$ or 0.87055. Its maximum value is unity. Thus, to a good approximation, the sphere of influence is foreshortened along $\bar{R}_2$ to 87% of its maximum value. Note that C is independent of k, and, therefore, the sphere of influence can never approach a true sphere.

For the various sun-planet systems, ρ is on the order of 10^{-3}, and Eq. (8) can be assumed to be a reasonable representation. For the earth-moon system, however, it is about 0.15, and Eq. (8) is not adequate.

In Fig. 2, the value of C is shown. For the planetary systems, one can find the radius of the sphere at any point by multiplying the appropriate value of C by the maximum radius in Table 1. The size and shape of the moon's sphere of influence, as determined from Eq. (5), is shown in Fig. 3. For comparison, the dashed curve also gives the result using Eq. (8). It is interesting that the shape given by (5) seems to be the same as that from (8) but is offset away from the Earth by about 4500 miles.

Table 1 Maximum radius of sphere of influence

System	ρ_{max}	r_{max}, miles
Earth-Moon	1.7211×10^{-1}	41,110
Sun-Venus	5.7038×10^{-3}	383,517
Sun-Earth	6.1817×10^{-3}	574,633
Sun-Mars	2.5352×10^{-3}	359,081

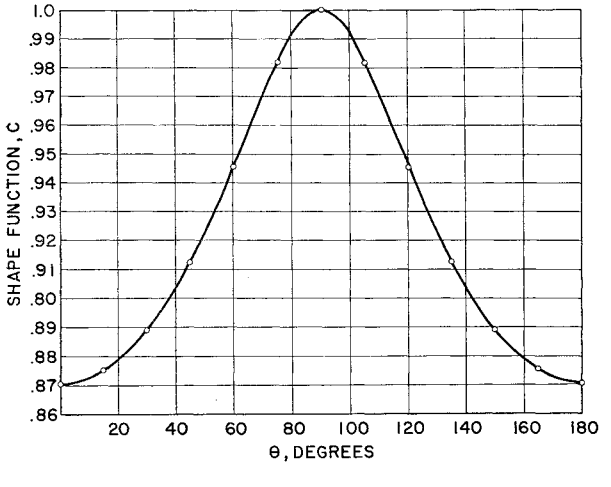

Fig. 2 Approximate shape function, from Eq. (8).

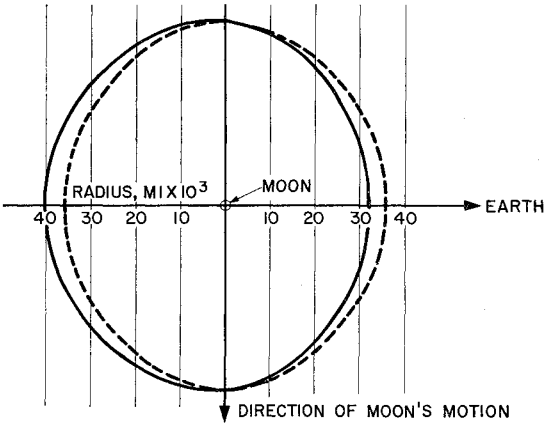

Fig. 3 The sphere of influence of the moon. Solid curve is the exact figure, from Eq. (5). Dashed curve, the approximate one, is obtained using the shape function of Fig. 2.

References

[1] Yegorov, V. A., "The capture problem in the three-body restricted orbital problem," NASA Tech. Transl. F-9 (April 1960).

[2] Subbotin, M. F., "Kurs nebesnoy mekhaniki," Vol. II, pp. 108–109, ONT 1 (1937).

[3] Notes on space technology, unpublished compilation by the Flight Research Div., NASA Langley Research Center (February 1958).

[4] Buchheim, R. W., "Motion of a small body in earth-moon space," Rand Corp. Res. Memo. RM-1726 (June 1956).

[5] Lieske, H. A., "Accuracy requirements for trajectories in the earth-moon system," Rand Corp. Rept. P-1022 (February 1957).

[6] Clement, G. H., "The moon rocket," Rand Corp. Rept. P-833 (May 1956).

[7] Lieske, H. A., "Lunar instrument carrier-trajectory studies," Rand Corp. Res. Memo. RM-1728 (June 1956).

[8] Buchheim, R. W., "Artificial satellites of the moon," Rand Corp. Rept. P-873 (June 1956).

[9] Plummer, H. C., *An Introductory Treatise on Dynamical Astronomy* (Dover Publications, New York, 1960, orig. publ. 1918), pp. 234–235.

[10] Lorell, J. and Oster, C., "A patched-conic computation program for interplanetary trajectories," Jet Propulsion Lab. Memo. 30-10 (September 1959).

[11] Crenshaw, J. W., "The sphere of influence in patched-conic methods," General Electric Missile and Space Div. Tech. Info. Ser. 62SD229 (December 1962).

Constraint Factor of Notched Bars by d.c.-Board

NOBUO INOUE* AND HARRY C. STUTTS†
Purdue University, Lafayette, Ind.

A d.c.-board and its accompanying measuring instruments for solving statically determinate problems in plasticity are described. A radial flow problem, to which an exact solution is known, is used to test the theory basic to this approach, showing the validity of the theory. By applying the d.c.-board technique, the collapse load of notched bars in tension was estimated. The results are compared with theoretical results using truncated wedge stress field and with actual test data.

Nomenclature

a = width of notched section
b = half length of notch
d = width of bar
E = electric-field intensity
I = electric-current intensity
I_x, I_y = electric-current components across the bar thickness per unit normal length
k = yield stress in pure shear
L = load
R = resistance
V = voltage

Subscript

$*$ = a reference value

A D.C.-BOARD for plastic states of stress introduced in a previous paper[1] was set up at the Aerospace Sciences Laboratory of the School of Aeronautical and Engineering Sciences, Purdue University. It resembles a patch board used in conjunction with analog computers in that its sole purpose is that of a receptacle, holding variable potentiometers in a prescribed pattern. The board was set up in a rectangular pattern and fitted with jacks so the potentiometers could be set at a desired value and placed anywhere on the board. The potentiometers used fell into three categories: 0–15, 0–30, and 0–1000 kohm. The smaller potentiometers were used as the body of the geometric representation of the configuration being considered. As many as 180 of these potentiometers were in use at one time on one problem. The 0–30-kohm potentiometers were used for those points that required higher than 15-kohm resistance. These points were few and consisted mainly of the symmetry line where the normal resistance was doubled. The largest potentiometers were used to obtain satisfactory boundary conditions. Figure 1 shows the apparatus which is set up for a typical notched bar problem, and the following describes this apparatus. The potentiometers (A) were adjusted by means of a General Radio Company type 650-A impedance bridge (B) to which was connected an external Leeds and Northrup 2430-A galvanometer (C). This equipment gave a maximum error of 2% in setting the potentiometers. A Beckman model 4011 digital voltmeter (D) was used to measure the potential at different points on the d.c.-board. This instrument had an accuracy of 0.01%. The radial flow problem[2] in plasticity was used to test the validity of the d.c.-board techniques, since an exact solution is available for this problem. The maximum error encountered was 1.35%.

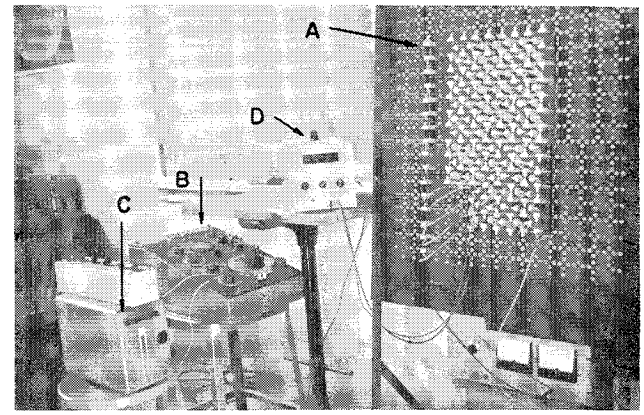

Fig. 1 Apparatus set up for a typical notched bar problem.

The notched bar problem was set up on d.c.-board. Because of symmetry, only one-fourth of the bar had to be placed on the d.c.-board, and the outside edge of the bar was connected to the positive side of 100 v while the centerline of the bar was grounded. Figure 1 shows a typical notched bar problem on the d.c.-board. The procedure for solving the problem was as follows. All potentiometers were initially set at 5 kohm except along the line of symmetry where the value was 10 kohm. The 1000-kohm potentiometers were adjusted, at near maximum value, so that a constant potential occurred across each of the 5-kohm potentiometers on the outside edge of the bar. This procedure resulted in a constant current I_* along the outside edge of the bar, which satisfied the boundary conditions. However, at the corner of the notch where two of the 5-kohm potentiometers join together at the boundary (since current is a vector), I_* had to be multiplied by $\frac{1}{2}^{1/2}$, and this new value of the current applied to each of these two potentiometers. Since the current was never measured directly but always was calculated from $I = E/R$, the voltage across these potentiometers was adjusted to be $\frac{1}{2}^{1/2}$ times the voltage across the rest of the outside potentiometers. Also, since the symmetry line had double resistance, the current across the outside potentiometer was equal to $I_*/2$. Once the boundary conditions had been set, neither the 1000-kohm potentiometers nor the potentiometers on the outside edge of the bar were ever adjusted again. The basic equations to the plane strain problem are given in Eq. (9) of the previous paper,[1] and it was found that by plotting the value of each potentiometer on Fig. 1 (field-intensity resistance relation) of the previous paper[1] a clearer picture resulted as to what adjustments needed to be made. R_* was fixed at 5 kohm, and I_* was a constant given by the boundary current. The resistance R was measured by the impedance bridge, thus leaving the current I as the only unknown. It must be remembered that current is a vector, and it has, therefore, both horizontal (I_x) and vertical (I_y) components, where $I = (I_x^2 + I_y^2)^{1/2}$. I_x is the current flowing through a potentiometer lying in the horizontal position, and I_y is the average current through the vertical potentiometers adjacent to it. A similar situa-

Received April 18, 1963; revision received June 24, 1963.

* Visiting Professor, School of Aeronautical and Engineering Sciences; on leave from Doshisha University, Kyoto, Japan. Member AIAA.

† Graduate Student, School of Aeronautical and Engineering Sciences; now with Analytic Services Inc., Bailey's Crossroads, Va.